Total absorption spectroscopy of the β decay of ^{76}Ga

A. C. Dombos,[1,2,3,*] D.-L. Fang,[1,3,4] A. Spyrou,[1,2,3] S. J. Quinn,[1,2,3] A. Simon,[1,5] B. A. Brown,[1] K. Cooper,[1,6] A. E. Gehring,[1,†] S. N. Liddick,[1,6] D. J. Morrissey,[1,6] F. Naqvi,[1,3] C. S. Sumithrarachchi,[1] and R. G. T. Zegers[1,2,3]

[1]*National Superconducting Cyclotron Laboratory, Michigan State University, East Lansing, Michigan 48824, USA*

[2]*Department of Physics and Astronomy, Michigan State University, East Lansing, Michigan 48824, USA*

[3]*Joint Institute for Nuclear Astrophysics, Michigan State University, East Lansing, Michigan 48824, USA*

[4]*College of Physics, Jilin University, Changchun, 130012, China*

[5]*Department of Physics and the Joint Institute for Nuclear Astrophysics, University of Notre Dame, Notre Dame, Indiana 46556, USA*

[6]*Department of Chemistry, Michigan State University, East Lansing, Michigan 48824, USA*

(Received 7 April 2016; published 17 June 2016)

The β decay of ^{76}Ga was studied using the technique of total absorption spectroscopy for the first time. The experiment was performed at the National Superconducting Cyclotron Laboratory using the Summing NaI(Tl) detector. The extracted β-decay feeding intensity distribution and Gamow-Teller transition strength distribution are compared to shell-model calculations to help constrain nuclear matrix elements relevant to the neutrinoless double-β decay of ^{76}Ge.

DOI: 10.1103/PhysRevC.93.064317

I. INTRODUCTION

Nuclear masses and the pairing interaction conspire in certain isobaric chains to create a scenario in which single-β decay is energetically forbidden while double-β decay is energetically allowed. If, in the latter process, two electrons and no neutrinos are emitted, this process is called neutrinoless double-β ($0\nu\beta\beta$) decay and denoted as ${}^{A}_{Z}X_{N} \rightarrow {}^{A}_{Z+2}Y_{N-2} + 2e^{-}$. An observation of $0\nu\beta\beta$ decay would demonstrate the violation of conservation of total lepton number and establish that neutrinos are Majorana particles as opposed to Dirac particles [1,2].

The even-even nucleus ^{76}Ge is a promising $0\nu\beta\beta$-decay candidate for many experimental reasons. The $Q_{\beta\beta}$ value ($Q_{\beta\beta} = 2039.061 \pm 0.007$ keV) [3] of this nucleus places the region of interest above many, but not all, sources of background. In addition, this nucleus is easily compatible with the existing experimental technique of using high-purity germanium detectors, which increases the signal-to-noise ratio due to the excellent energy resolution provided by these types of detectors. While $0\nu\beta\beta$ decay has never been observed in any nucleus, the search for this process remains steadfast. Highly sensitive experiments performed by multinational collaborations such as the Heidelberg-Moscow experiment [4], the International Germanium Experiment (IGEX) [5,6], and the Germanium Detector Array (GERDA) phase I [7] have placed lower limits on the half-life of ^{76}Ge $0\nu\beta\beta$ decay. The next generation of experiments of GERDA phase II [8] and MAJORANA [9] are devoted to observing and measuring the half-life of $0\nu\beta\beta$ decay in ^{76}Ge, or, if no observation is made, placing a strong lower limit on the half-life.

Together with experimental efforts, theory has focused on calculating nuclear matrix elements necessary for $0\nu\beta\beta$ decay in ^{76}Ge [1]. The nuclear matrix elements are important because they are needed to calculate the decay rate for $0\nu\beta\beta$ decay, denoted as $(T^{0\nu}_{1/2})^{-1}$, assuming the theoretical description is given by light neutrino exchange, as [1]

$$\left(T^{0\nu}_{1/2}\right)^{-1} = G_{0\nu}|M_{0\nu}|^2\langle m_{\beta\beta}\rangle^2, \tag{1}$$

where $G_{0\nu}$ is the phase space factor [10–13], $M_{0\nu}$ is the nuclear matrix element, and $\langle m_{\beta\beta}\rangle$ is the effective mass of the neutrino. According to Eq. (1), the nuclear matrix elements can be used with current lower limits on the half-life to provide upper limits on $\langle m_{\beta\beta}\rangle$ or extract $\langle m_{\beta\beta}\rangle$ if the half-life is eventually measured.

The nuclear matrix elements have been calculated using different nuclear structure models, and for a given nucleus can be quite uncertain [14,15]. Three models which have provided recent calculations relevant to ^{76}Ge are the shell model [16], quasiparticle random-phase approximation (QRPA) [17], and the interacting boson model (IBM-2) [18]. These three models were recently compared to one another for the case of ^{76}Ge and deficiencies were found in all three models [19], a problem that is common to all $0\nu\beta\beta$-decay candidates.

In this paper, we provide new experimental data in the $A = 76$ mass chain that can be compared to some of the aforementioned theoretical calculations. This is done by measuring the β-decay feeding intensity distribution of ^{76}Ga as a function of excitation energy in the daughter nucleus ^{76}Ge. Since the β-decay feeding intensity distribution is sensitive to the wave functions of the ground state of the parent and those of the populated daughter states, the measurement can be used to test the nuclear structure models which are used to calculate the nuclear matrix elements. We extract the β-decay feeding intensity distribution using the technique of total absorption spectroscopy (TAS) [20], which avoids problems posed by the Pandemonium effect [21]. The Pandemonium effect appears when attempting to measure the β-decay feeding intensity distribution using detectors that are designed for good energy resolution but suffer from poor efficiency. These detectors may miss some of the low-intensity and/or high-energy γ rays

*dombos@nscl.msu.edu

†Present address: Neutron Science and Technology Group, Los Alamos National Laboratory, Mail Stop H803, Los Alamos, NM 87545.

and as a result the β-decay feeding intensity distribution is artificially enhanced at low excitation energies. The method of using total absorption spectroscopy to learn about the structure of the ground state of the parent nucleus has been successfully performed in the past (for example, Refs. [22–26]).

In addition to β-decay studies with the TAS technique, charge-exchange reactions can also be used for the study of the Gamow-Teller transition strength distribution. One recent experiment relevant to the $A = 76$ mass chain used the ^{76}Ge(^{3}He,t)^{76}As charge-exchange reaction to extract the Gamow-Teller transition strength distribution of ^{76}Ge as a function of excitation energy in ^{76}As [27]. The extracted Gamow-Teller transition strength distribution was highly fragmented, which was interpreted as resulting from nuclear structure effects of the $A = 76$ system. In Ref. [28], this experimental distribution was compared to that obtained from a theoretical model in order to validate their calculations of nuclear matrix elements relevant to $0\nu\beta\beta$ decay.

In the present work, the β-decay feeding intensity distribution and Gamow-Teller transition strength distribution were measured through the β decay of ^{76}Ga. The experimental details are presented in Sec. II, the analysis procedure is described in Sec. III, and the results and comparison to theory are presented in Sec. IV.

II. EXPERIMENTAL DETAILS

The experiment was performed at the National Superconducting Cyclotron Laboratory (NSCL) at Michigan State University. The Coupled Cyclotron Facility produced a primary beam of ^{76}Ge $^{32+}$ with an energy of 130 MeV/u, which was impinged on a ^{9}Be production target that had a thickness of 399 mg/cm^2. Using a 184 mg/cm^2 Al wedge, the A1900 fragment separator [29] created a secondary beam with a momentum acceptance of 0.5% of approximately 73% of ^{76}Ga $^{31+}$ (the isotope of interest) and 27% of ^{74}Zn $^{30+}$.

After the A1900 fragment separator, the secondary beam was sent to the NSCL gas stopping station [30], which partly consists of a solid degrader system, linear gas cell or gas catcher, and extraction system. The solid degrader system consisted of a 1555-μm Al degrader and a 1045-μm silicon dioxide wedge to remove nearly all of the kinetic energy and spread in kinetic energy of the secondary beam before entering the gas cell, respectively. By changing the angle of the degrader, primarily ^{76}Ga $^{31+}$ was stopped in the gas cell after passing through a thin Al window. The secondary beam was thermalized in the gas cell and subsequently extracted. A scan of the activity as a function of mass of the ions extracted from the gas cell revealed the molecular ion $[^{76}Ga(H_2O)]^+$ to be the most common, and this was delivered to the experimental end station.

The experimental end station consisted of the Summing NaI(Tl) (SuN) detector [31] and a small silicon surface barrier detector installed inside the bore hole of SuN. SuN is a segmented total absorption spectrometer that is optimized for geometric and intrinsic efficiency and is an ideal detector for performing total absorption spectroscopy. SuN is a right-circular cylindrical detector that is 16 in. in diameter and 16 in. in length, has a 1.8-in.-diameter bore hole along the beam axis, and can separate into a top half and bottom half in order to fit around the beam line. Each half consists of four optically isolated segments, and each segment contains a large NaI crystal that is read out by three photomultiplier tubes (PMTs). The NSCL Digital Data Acquisition System (DDAS) [32] is used to record signals in SuN. Together, the large summing efficiency and relatively good energy resolution for a scintillator [85(2)% efficiency and an average segment resolution of 6.1(2)% for the 661-keV γ ray from the decay of ^{137}Cs] make SuN ideally suited for these types of experiments. In front of the silicon surface barrier detector was a rectangular aluminum frame that was 0.5 mm thick, which held a thin aluminum foil. The ^{76}Ga ions, which had an energy of approximately 40 keV and intensity of approximately 500 particles per second, were implanted into the aluminum target foil. The electrons from the β decay of ^{76}Ga were detected in the silicon surface barrier detector in coincidence with the β-delayed γ rays in SuN.

First results from this experiment were already published in Ref. [33] where the so-called β-Oslo technique was introduced.

III. ANALYSIS

Before the start of the experiment, the PMTs of SuN were gain matched by adjusting the high voltage applied to each PMT. The high voltage was adjusted until the 1460.8-keV γ ray from the decay of ^{40}K that is present in the room background appeared at the same channel number for each PMT. Then the PMTs and segments of SuN were further gain matched and calibrated, respectively, in software with the following procedure. First, the PMTs were gain matched by applying a multiplication factor to the energy of each outer PMT so that the ^{40}K peak appeared at the same channel number as the corresponding peak in the central PMT within a given segment. Then the energy of all three PMTs for a given segment were added together to determine the energy deposition within that segment. An individualized quadratic calibration was then applied to each segment so that γ rays were located at the correct energy. For this analysis, the calibration used the 563-, 1108-, and 3952-keV γ rays, which are emitted following the β decay of ^{76}Ga. Finally, the energy of all eight segments were added together to create the TAS spectrum (an energy threshold of 80 keV was applied to each segment before being added to the TAS spectrum). Due to the energy threshold applied to each segment, the TAS spectrum will naturally have an energy threshold of 80 keV as well. Because the location of a so-called sum peak in the TAS spectrum has a dependence on the multiplicity of the γ-ray decay cascade (due to the nonproportional light yield in a NaI(Tl) crystal [34]), a multiplicity-dependent correction factor was applied to the TAS spectrum.

In addition to the TAS spectrum, the segmentation of SuN provides two additional spectra that can be used to extract the β-decay feeding intensity distribution. The first spectrum is the so-called sum-of-segments spectrum, which is created by treating each segment of SuN as an independent detector that detects the individual γ rays in a decay cascade. For each event, the *counts* from all eight segments are added together (as

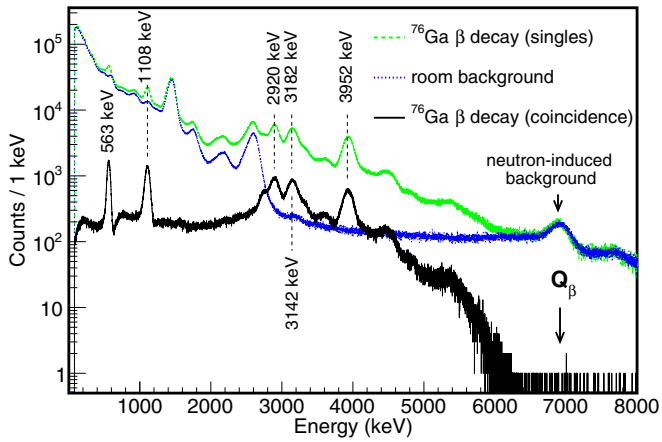

FIG. 1. The TAS spectrum of SuN for the β decay of ^{76}Ga in singles (green, dashed line), normalized room background (blue, dotted line), and with a coincidence requirement with the silicon surface barrier detector (black, solid line). The energies of prominent sum peaks are labeled in the coincidence spectrum. There is also a label for the Q value for the β decay of ^{76}Ga at 6916.2(2.0) keV [35].

opposed to the TAS spectrum, which is created by adding the *energy* of all eight segments for an event). The second spectrum is the multiplicity spectrum (also referred to as the hit pattern [31]), which is the number of segments that detect energy during the decay cascade. A lower (higher) γ multiplicity of the actual decay cascade corresponds to a lower (higher) number of segments that detected energy in the multiplicity spectrum.

There were no external trigger requirements to record data in the experiment. Comparing the TAS spectrum of normalized room background (blue, dotted line in Fig. 1) to the TAS spectrum of the β decay of ^{76}Ga in singles mode (green, dashed line in Fig. 1) reveals that the lower energies are dominated by room background. Subtracting the two spectra to create a TAS spectrum corresponding purely to the β decay of ^{76}Ga would create significant statistical fluctuations. Instead, the background radiation was removed by adding a coincidence requirement between a β-decay electron in the silicon surface barrier detector and β-delayed γ rays in SuN, producing a so-called β-gated TAS spectrum (black, solid line in Fig. 1). The TAS spectrum with the coincidence requirement shows significant suppression of the background radiation, no issues from beam-induced background, and clearly visible sum peaks. For example, the first excited state in ^{76}Ge occurs at 563 keV, the second excited state occurs at 1108 keV, and some of the higher-energy excited states that have a relatively large β-decay feeding intensity occur at 2920, 3142, 3182, and 3952 keV.

The β-gated TAS spectrum was used to extract the β-decay feeding intensity distribution. The distribution was extracted with a combination of a folding procedure and χ^2 minimization. The folding procedure used the detector response function of SuN, which was modeled with GEANT4 [36]. The detector response function of SuN has been verified by comparing experimental and simulated spectra for standard calibration sources such as ^{60}Co and ^{137}Cs [31], and resonances for the ^{27}Al(p,γ)^{28}Si reaction [31].

The detector response function of SuN was used to simulate each decay cascade from the existing decay scheme for the β decay of ^{76}Ga [37] from the National Nuclear Data Center (NNDC). Each decay cascade had a corresponding TAS spectrum, sum-of-segments spectrum, and multiplicity spectrum. The conditions imposed on the simulated spectra of these decay cascades were identical to those imposed on the experimental spectra, such as the energy threshold applied to each SuN segment, as well as the same coincidence requirement with the silicon surface barrier detector by including β-decay electrons that have a kinetic energy distribution modified by a Fermi function [38].

The simulated spectra from all the decay cascades were used to minimize the global χ^2:

$$\chi^2_{\text{global}} = \sum_i \sum_j \left(\frac{e_{ij} - s_{ij}}{\sqrt{e_{ij}}} \right)^2, \tag{2}$$

where the index i runs over all spectra included in the fit, the index j runs over all bins included in the fit, and e_{ij} and s_{ij} are the contents of spectrum i at bin j for experiment and simulation, respectively. The TAS spectrum, sum-of-segments spectrum, and multiplicity spectrum were fit simultaneously. Including these two latter spectra is important because the efficiency of SuN to produce a count in the TAS spectrum depends on the energy of the individual γ rays and multiplicity of the decay cascade, information that is contained in the sum-of-segments spectrum and multiplicity spectrum, respectively. The quantity s_{ij} is affected by many different decay cascades and therefore, for a given i, is defined as

$$s_{ij} = \sum_k p_k c_{jk}, \tag{3}$$

where the index k runs over all simulated decay cascades, p_k is the probability for a particular decay cascade, and c_{jk} is the content of bin j produced by decay cascade k. The probabilities were continuously varied until χ^2_{global} was minimized. Note that the probabilities in Eq. (3) are the β-decay feeding intensity to a particular level multiplied by the probability for a specific decay cascade from that level to the ground state. Because the probabilities of all decay cascades from a level to the ground state must sum to unity, the sum of p_k for a given level is the β-decay feeding intensity to that level.

If the experimental spectra were not reproduced with the χ^2 minimization procedure using decay cascades from the existing decay scheme, then modifications were made by adding so-called pseudo levels to the existing decay scheme. In theory, a pseudo level is placed at a specific excitation energy in the existing decay scheme, but in reality acts as a representative for all nearby levels within the energy resolution of SuN. Since all the possible ways that a pseudo level can de-excite to the ground state are unknown, transitions to all levels in the existing decay scheme were included in the fitting process.

Comparing the experimental and simulated spectra using the existing decay scheme reveals that even though ^{76}Ga is only one unit away from stability, the existing decay scheme is not well known (Fig. 2). Indeed, the existing decay scheme suffers from typical symptoms of the Pandemonium effect: In general, there is an overestimation of the β-decay feeding

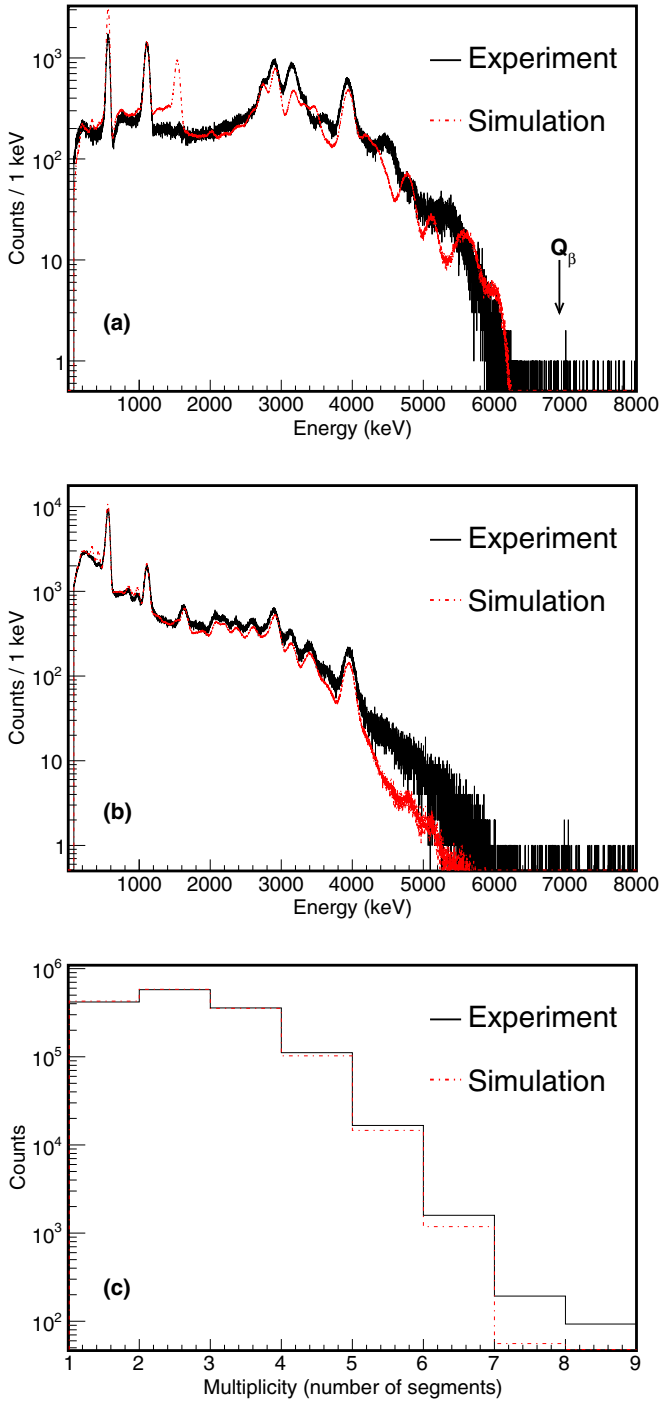

FIG. 2. Comparison of experimental (black, solid line) and simulated (red, dashed-dotted line) spectra using the existing decay scheme [37] to illustrate the discrepancy with the measurements reported in the present work. The spectra are (a) the TAS spectrum, (b) sum-of-segments spectrum, and (c) multiplicity spectrum. All three spectra were created with an energy threshold of 80 keV applied to each SuN segment. There is a label for Q value in the TAS spectrum for the β decay of ^{76}Ga at 6916.2(2.0) keV [35].

intensity at lower excitation energies and an underestimation of the β-decay feeding intensity at higher excitation energies; in particular, the 1539-keV level that was previously observed in

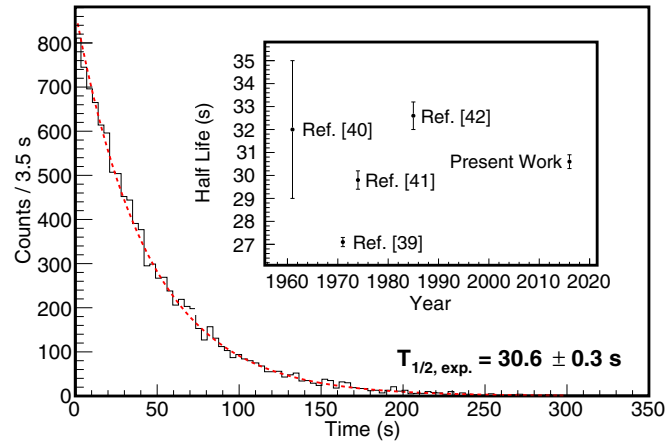

FIG. 3. The experimental decay curve for the β decay of ^{76}Ga (black, solid line) and the exponential fit from 0 to 300 s (red, dashed line). The extracted half-life is 30.6(3) s. The inset show the history of measurements of the half-life of ^{76}Ga.

a high-resolution experiment to have a relatively large β-decay feeding intensity [39] is negligible in the present measurement.

In order to reproduce the experimental spectra, the β-decay feeding intensity to existing levels was adjusted. In addition, three pseudo levels were added to the existing decay scheme at 4600, 4950, and 5350 keV.

IV. RESULTS

A. Half-life

The β-decay half-life of ^{76}Ga was measured by turning the beam off and measuring the implanted activity as a function of time. This allows one to create a decay curve, shown in Fig. 3, from which the half-life can be extracted. The decay curve is a histogram of time differences between the beginning of the run (beam off) and when a β-decay electron is registered in the silicon surface barrier detector. The decay curve between 0 and 300 s was fit using an exponential function. A half-life of 30.6(3) s was obtained for the β decay of ^{76}Ga, in reasonably good agreement with previous measurements. The half-life of ^{76}Ga has been measured four times in the past: Ref. [40] used fast neutron bombardment on natural Ge to produce ^{76}Ga via a (n,p) reaction and obtained a half-life of 32(3) s; Ref. [39] used a (n,p) reaction on a GeO_2 target (enriched to 73.89% in ^{76}Ge) to produce ^{76}Ga and obtained a half-life of 27.1(2) s; Ref. [41] produced ^{76}Ga from fission and obtained a half-life of 29.8(4) s; and Ref. [42] created ^{76}Ga with a (n,p) reaction on Ge metal (enriched to 92.82% in ^{76}Ge) and obtained a half-life of 32.6(6) s.

B. Total absorption spectroscopy

The TAS spectrum, sum-of-segments spectrum, and multiplicity spectrum were fit simultaneously in order to extract the β-decay feeding intensity distribution. Systematic uncertainties coming from the energy calibration and binning were taken into account and the final β-decay feeding intensity distribution in Table I is an average of all the fits with

TABLE I. The β-decay feeding intensity distribution of ^{76}Ga as a function of excitation energy in the daughter nucleus ^{76}Ge. Intensity values below 10^{-4}% are set to 0.

Energy (keV)	Intensity (%)	Error (−)	Error (+)	Energy (keV)	Intensity (%)	Error (−)	Error (+)
563	7.3	0.2	0.2	3887	3	1	1
1108	11.7	0.9	0.9	3952	12	1	1
1410	0.34	0.04	0.04	4122	1.4	0.2	0.2
1539	0.5	0.1	0.1	4193	1.2	0.2	0.2
1911	0.21	0.04	0.04	4239	0.04	0.04	0.05
2020	0.11	0.05	0.04	4327	2.4	0.4	0.3
2591	1.1	0.3	0.3	4364	0.1	0.1	0.3
2655	0			4477	2.3	0.3	0.3
2692	0.6	0.4	0.4	4600	3.4	0.6	0.6
2748	5.4	0.9	0.9	4720	0.31	0.07	0.06
2769	0			4784	0.54	0.09	0.09
2842	3.9	0.4	0.4	4813	0		
2920	9.8	0.9	0.9	4815	0.6	0.1	0.1
3142	9	1	1	4950	1.1	0.3	0.2
3182	7.4	0.9	0.9	5122	0.7	0.1	0.1
3232	0.7	0.2	0.2	5350	1.6	0.3	0.3
3312	1.8	0.2	0.2	5523	0.7	0.2	0.2
3323	2.9	0.3	0.3	5663	0.7	0.3	0.3
3335	0.2	0.2	0.2	5750	0.19	0.08	0.08
3409	0.24	0.04	0.04	5883	0.2	0.2	0.2
3478	1.6	0.2	0.2	6021	0.03	0.03	0.1
3633	2.8	0.4	0.4	6065	0.1	0.1	0.1

the aforementioned different fitting conditions of the energy calibration and binning. An example of one of those fitting conditions with a specific energy calibration and binning is shown in Fig. 4.

Three different sources of uncertainty contribute to the total uncertainty that is reported in Table I. The first source of uncertainty comes from fitting with different conditions. For each excitation energy, the minimum, average, and maximum intensity of the different fitting conditions was calculated. The difference between the average and the minimum (maximum) intensity contributes to the lower (upper) bound on the uncertainty. The weighted average of the uncertainty from different fitting conditions was 6%. The second source of uncertainty comes from the statistics of the TAS spectrum. The inherent statistical uncertainty in the number of counts per bin in the TAS spectrum is directly related to the uncertainty in the extracted β-decay feeding intensity distribution. The weighted average of the uncertainty from statistics was also 6%. The third source of uncertainty is from the efficiency of SuN. The efficiency of SuN depends on the multiplicity of the γ decay cascade and on the energy of the individual γ rays. The procedure described in Ref. [31] was used to estimate the uncertainty in the efficiency. The weighted average of the uncertainty from summing efficiency was 9%.

C. Theory

The ground state and β-decay properties of ^{76}Ga were calculated with the shell model. The calculations were performed with the NUSHELLX@MSU code [43]. The *jj44* model space

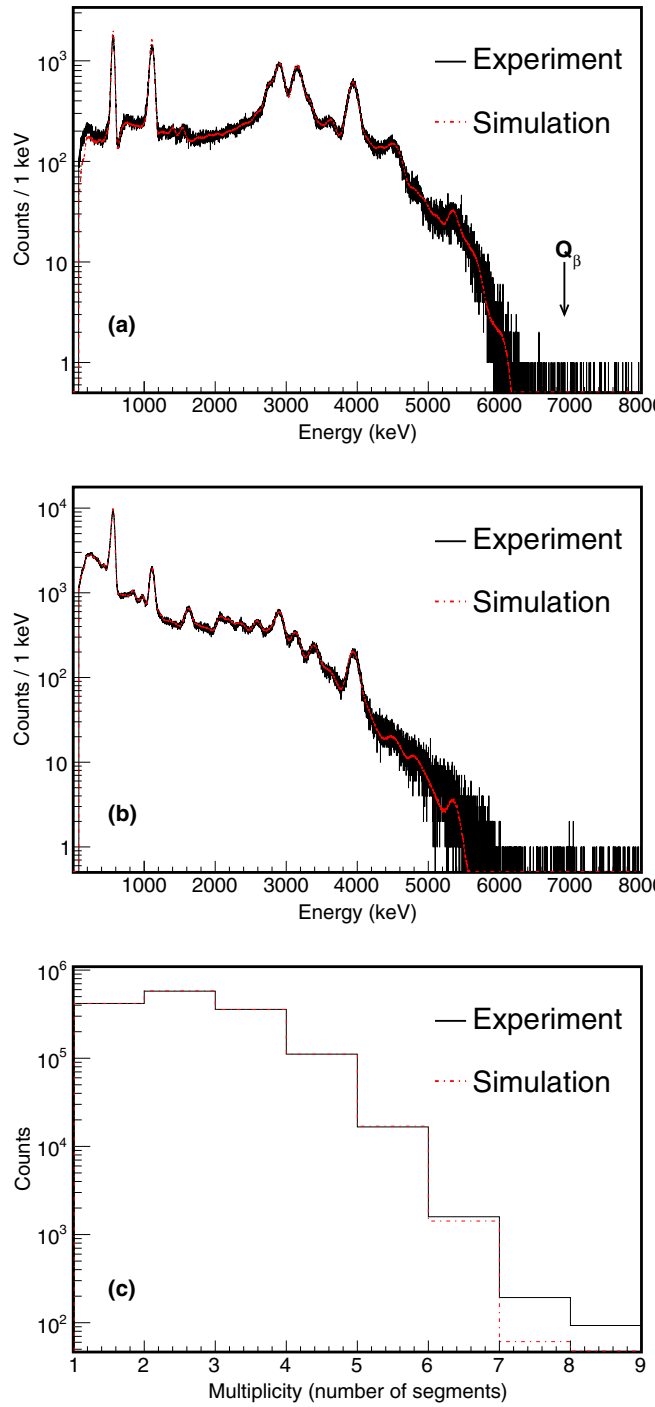

FIG. 4. Comparison of experimental (black, solid line) and simulated (red, dash-dotted line) spectra after fitting all three spectra simultaneously with the decay scheme modifications for (a) the TAS spectrum, (b) sum-of-segments spectrum, and (c) multiplicity spectrum. This is an example of one of the different fitting conditions with a specific energy calibration and binning. All three spectra were created with an energy threshold of 80 keV applied to each SuN segment. There is a label for Q value in the TAS spectrum for the β decay of ^{76}Ga at 6916.2(2.0) keV [35].

was used, which has an inert core of ^{56}Ni and active nucleons in the $0f_{5/2}, 1p_{1/2}, 1p_{3/2}$, and $0g_{9/2}$ single-particle orbitals for

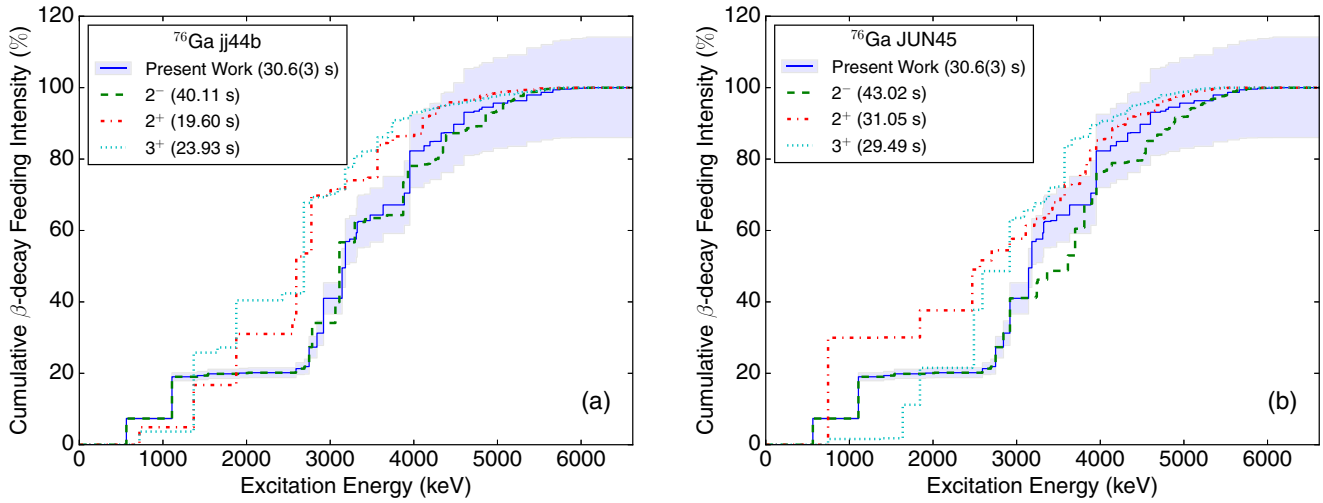

FIG. 5. Cumulative β-decay feeding intensity of ^{76}Ga as a function of excitation energy in the daughter nucleus ^{76}Ge for the present work (blue, solid line, with uncertainty in light-blue shading) and calculations with different Hamiltonians and different assumptions of the spin and parity of the ground state of ^{76}Ga. Panel (a) contains calculations using the *jj*44b Hamiltonian and panel (b) contains calculations using the JUN45 Hamiltonian. The half-lives from the present work and theoretical calculations are in parentheses. For the present work, the blue solid line is the cumulative average intensity, and the lower (upper) bound of the light-blue uncertainty band is the cumulative minimum (maximum) intensity. See text for an explanation of why the 2^- calculation and the present work are identical at relatively low excitation energy.

both protons and neutrons. Two Hamiltonians were used: the JUN45 Hamiltonian [44] and the *jj*44b Hamiltonian [45].

The NNDC [37] lists $(2^+, 3^+)$ for the spin and parity of the ground state of ^{76}Ga, while a measurement of the magnetic moment [46] prefers a 2^- assignment when compared to shell-model calculations. With the JUN45 Hamiltonian there are 11 states below 300 keV in ^{76}Ga with spins $(1–5)^-$ and 2^+. Due to the uncertainty in the energy of the states, the Hamiltonians are unable to predict the spin and parity of the ground state in this situation. Thus, the theoretical β decay for $(2^+, 3^+)$ and 2^- were considered and compared with the experiment. Shown in Fig. 5 is the cumulative β-decay feeding intensity of ^{76}Ga as a function of excitation energy in the daughter nucleus ^{76}Ge. Figure 5 contains the measurement from the present work, along with theoretical calculations using the two Hamiltonians and different assumptions of the spin and parity of the ground state of ^{76}Ga. Calculating the first-forbidden (FF) β-decay transitions in the *jj44* model space is not practical since most of the FF one-body transitions lie outside the model space (only the $0f_{5/2}$ to $0g_{9/2}$ is inside). The results for the two Hamiltonians in Fig. 5 generally agree with each other but differ on the detailed spectra for the daughter nucleus ^{76}Ge. Based on a comparison of experimental β^--decay half-lives with those calculated with these Hamiltonians in the *jj44* model space a quenching factor of $g_A = 0.4g_{A_0}$ is required [47]. This quenching factor of $g_A = 0.4g_{A_0}$ was applied to both Hamiltonians. This is a larger quenching than the typical value of $g_A \approx 0.7g_{A_0}$ found for the *sd* and *pf* model spaces. The larger quenching is related to the fact that a large fraction of the β^- giant Gamow-Teller resonance lies outside *jj44* model space. The larger quenching approximately takes into account the coupling between the low-lying GT transitions to the missing part of the GT giant resonance.

The β-decay feeding intensity distribution can be converted to a Gamow-Teller transition strength distribution, B(GT), according to the equation,

$$B(\mathrm{GT})(E) = K\left(\frac{g_V}{g_A}\right)^2 \frac{I_\beta(E)}{f(Q_\beta - E)T_{1/2}}, \qquad (4)$$

where E is the excitation energy, $K = 6143.6(17)$ s [48], $g_A/g_V = -1.270(3)$ [49], I_β is the β-decay feeding intensity to a particular excitation energy, f is the Fermi integral corresponding to a particular excitation energy, Q_β is the ground state to ground state Q_β value, and $T_{1/2}$ is the half-life. The units of B(GT) using Eq. (4) are $g_A^2/4\pi$. In Eq. (4), the β-decay feeding intensity distribution from the present work was used for I_β, the half-life from the present work was used for $T_{1/2}$, and the Q_β value was taken from the 2012 Atomic Mass Evaluation [35]. The Fermi integrals were calculated numerically as explained in Ref. [50]. A comparison of the present work to shell-model calculations is shown in Fig. 6.

With these Hamiltonians, the states with negative parity in ^{76}Ge lie above 2.5 MeV. If the ground state of ^{76}Ga has positive parity, then the β-decay to states in ^{76}Ge below 2.5 MeV is GT. With a quenching factor of $g_A = 0.4g_{A_0}$ there is good agreement with the experimental half-life especially for the JUN45 interaction (see Figs. 5 and 6). When the ground state of ^{76}Ga has negative parity, all of the transitions to the low-lying positive parity states in ^{76}Ge are FF. In this case the experimental values of the β-decay feeding intensity and Gamow-Teller transition strength were used in place of a theoretical estimate up to a threshold of 2.8 MeV for the *jj*44b interaction and a threshold of 3 MeV for the JUN45 interaction. With this method the half-life for the 2^- decay obtained with the *jj*44b Hamiltonian agrees with experiment, bearing in mind that there may also be FF transitions above the thresholds. After combining the results of this work and that in Ref. [46], the *jj*44b Hamiltonian is somewhat preferred and the ground state of ^{76}Ga is likely 2^-.

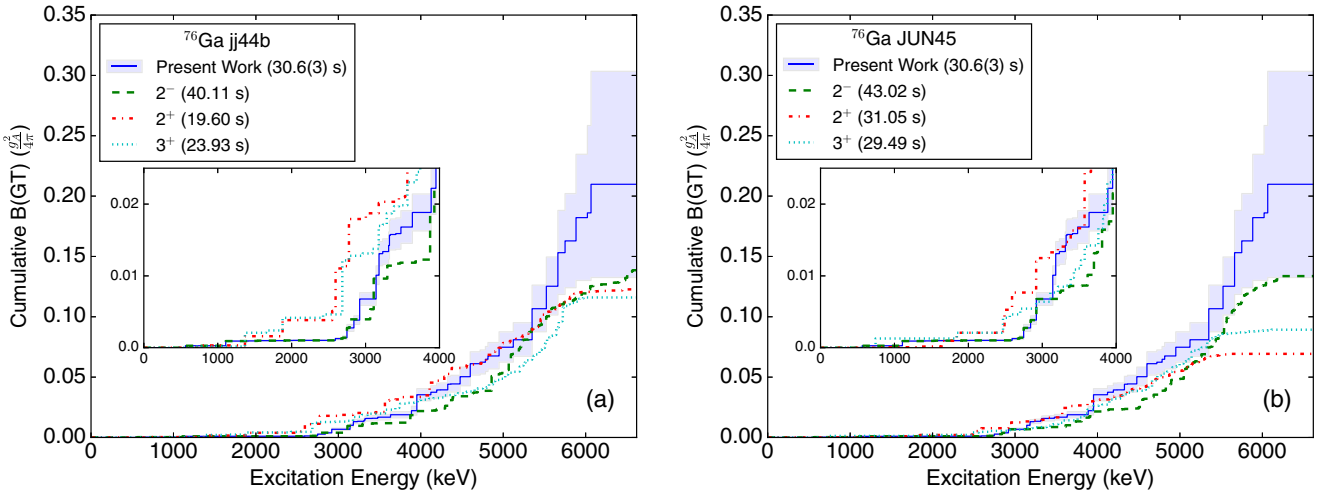

FIG. 6. Same as Fig. 5, but for cumulative B(GT). The inset shows a closeup view of the low-excitation energy region.

V. CONCLUSIONS

In an effort to provide experimental data that can be compared to theoretical models that are used to calculate nuclear matrix elements relevant to the neutrinoless double-β decay of ^{76}Ge, the β decay of ^{76}Ga was studied for the first time using the technique of total absorption spectroscopy with the SuN detector at the National Superconducting Cyclotron Laboratory. The measurement revises current values for the β-decay feeding intensity distribution found in the existing decay scheme at the National Nuclear Data Center since the existing decay scheme appears to have suffered from the Pandemonium effect. Regarding the theoretical calculations, the *jj*44b Hamiltonian does better than JUN45 for this particular decay for the assumed spin and parity of the ground state of ^{76}Ga. This is evident by the comparison to the β-decay feeding intensity distribution (Fig. 5), where *jj*44b can reproduce the data in the whole energy region. However, there are many nearly degenerate spin and parities predicted for ^{76}Ga and the experimental value for the ground state is not definite. The overall success of these two Hamiltonians will depend on their comparison to a wide range of data, which goes beyond the scope of this paper, which is the experimental results for the β decay of ^{76}Ga.

ACKNOWLEDGMENTS

This work was supported by the National Science Foundation under Grants No. PHY 1102511 (NSCL), No. PHY 1430152 (JINA-CEE), No. PHY 1350234 (CAREER), and No. PHY 1404442.

[1] F. T. Avignone, S. R. Elliott, and J. Engel, Rev. Mod. Phys. **80**, 481 (2008).
[2] J. D. Vergados, H. Ejiri, and F. Šimkovic, Rep. Prog. Phys. **75**, 106301 (2012).
[3] B. J. Mount, M. Redshaw, and E. G. Myers, Phys. Rev. C **81**, 032501 (2010).
[4] H. V. Klapdor-Kleingrothaus, A. Dietz, L. Baudis, G. Heusser, I. V. Krivosheina, B. Majorovits, H. Paes, H. Strecker, V. Alexeev, A. Balysh, A. Bakalyarov, S. T. Belyaev, V. I. Lebedev, and S. Zhukov, Eur. Phys. J. A **12**, 147 (2001).
[5] C. E. Aalseth *et al.* (IGEX Collaboration), Phys. Rev. D **65**, 092007 (2002).
[6] C. E. Aalseth, F. T. Avignone, R. L. Brodzinski, S. Cebrian, E. Garcia, D. Gonzales, W. K. Hensley, I. G. Irastorza, I. V. Kirpichnikov, A. A. Klimenko, H. S. Miley, A. Morales, J. Morales, A. Ortiz de Solorzano, S. B. Osetrov, V. S. Pogosov, J. Puimedon, J. H. Reeves, M. L. Sarsa, A. A. Smolnikov, A. S. Starostin, A. G. Tamanyan, A. A. Vasenko, S. I. Vasiliev, and J. A. Villar, Phys. Rev. D **70**, 078302 (2004).
[7] M. Agostini *et al.* (GERDA Collaboration), Phys. Rev. Lett. **111**, 122503 (2013).
[8] C. A. Ur, Nucl. Phys. B **217**, 38 (2011).
[9] N. Abgrall, E. Aguayo, F. T. Avignone III *et al.*, Adv. High Energy Phys. **2014**, 365432 (2014).
[10] J. Suhonen and O. Civitarese, Phys. Rep. **300**, 123 (1998).
[11] J. Kotila and F. Iachello, Phys. Rev. C **85**, 034316 (2012).
[12] S. Stoica and M. Mirea, Phys. Rev. C **88**, 037303 (2013).
[13] J. Kotila, J. Barea, and F. Iachello, Phys. Rev. C **91**, 064310 (2015).
[14] P. Vogel, J. Phys. G: Nucl. Part. Phys. **39**, 124002 (2012).
[15] A. Giuliani and A. Poves, Adv. High Energy Phys. **2012**, 857016 (2012).
[16] R. A. Sen'kov and M. Horoi, Phys. Rev. C **90**, 051301 (2014).
[17] D.-L. Fang, A. Faessler, V. Rodin, and F. Šimkovic, Phys. Rev. C **83**, 034320 (2011).
[18] J. Barea, J. Kotila, and F. Iachello, Phys. Rev. C **91**, 034304 (2015).
[19] B. A. Brown, D.-L. Fang, and M. Horoi, Phys. Rev. C **92**, 041301(R) (2015).
[20] C. L. Duke, P. G. Hansen, O. B. Nielsen, and G. Rudstam, Nucl. Phys. A **151**, 609 (1970).

[21] J. C. Hardy, L. C. Carraz, B. Jonson, and P. G. Hansen, Phys. Lett. B **71**, 307 (1977).
[22] E. Nácher, A. Algora, B. Rubio, J. L. Taín, D. Cano-Ott, S. Courtin, P. Dessagne, F. Maréchal, C. Miehé, E. Poirier, M. J. G. Borge, D. Escrig, A. Jungclaus, P. Sarriguren, O. Tengblad, W. Gelletly, L. M. Fraile, and G. Le Scornet, Phys. Rev. Lett. **92**, 232501 (2004).
[23] A. B. Pérez-Cerdán, B. Rubio, W. Gelletly, A. Algora, J. Agramunt, E. Nácher, J. L. Taín, P. Sarriguren, L. M. Fraile, M. J. G. Borge, L. Caballero, P. Dessagne, A. Jungclaus, G. Heitz, F. Marechal, E. Poirier, M. D. Salsac, and O. Tengblad, Phys. Rev. C **88**, 014324 (2013).
[24] M. E. Estévez Aguado, A. Algora, J. Agramunt, B. Rubio, J. L. Taín, D. Jordán, L. M. Fraile, W. Gelletly, A. Frank, M. Csatlós, L. Csige, Z. Dombrádi, A. Krasznahorkay, E. Nácher, P. Sarriguren, M. J. G. Borge, J. A. Briz, O. Tengblad, F. Molina, O. Moreno, M. Kowalska, V. N. Fedosseev, B. A. Marsh, D. V. Fedorov, P. L. Molkanov, A. N. Andreyev, M. D. Seliverstov, K. Burkard, and W. Hüller, Phys. Rev. C **92**, 044321 (2015).
[25] J. A. Briz, E. Nácher, M. J. G. Borge, A. Algora, B. Rubio, P. Dessagne, A. Maira, D. Cano-Ott, S. Courtin, D. Escrig, L. M. Fraile, W. Gelletly, A. Jungclaus, G. Le Scornet, F. Maréchal, C. Miehé, E. Poirier, A. Poves, P. Sarriguren, J. L. Taín, and O. Tengblad, Phys. Rev. C **92**, 054326 (2015).
[26] E. Poirier *et al.* (ISOLDE Collaboration), Phys. Rev. C **69**, 034307 (2004).
[27] J. H. Thies, D. Frekers, T. Adachi, M. Dozono, H. Ejiri, H. Fujita, Y. Fujita, M. Fujiwara, E.-W. Grewe, K. Hatanaka, P. Heinrichs, D. Ishikawa, N. T. Khai, A. Lennarz, H. Matsubara, H. Okamura, Y. Y. Oo, P. Puppe, T. Ruhe, K. Suda, A. Tamii, H. P. Yoshida, and R. G. T. Zegers, Phys. Rev. C **86**, 014304 (2012).
[28] R. A. Sen'kov and M. Horoi, Phys. Rev. C **93**, 044334 (2016).
[29] D. J. Morrissey, B. M. Sherrill, M. Steiner, A. Stolz, and I. Wiedenhoever, Nucl. Instrum. Methods Phys. Res., Sect. B **204**, 90 (2003).
[30] K. Cooper, C. S. Sumithrarachchi, D. J. Morrissey, A. Levand, J. A. Rodriguez, G. Savard, S. Schwarz, and B. Zabransky, Nucl. Instrum. Methods Phys. Res., Sect. A **763**, 543 (2014).
[31] A. Simon, S. J. Quinn, A. Spyrou, A. Battaglia, I. Beskin, A. Best, B. Bucher, M. Couder, P. A. DeYoung, X. Fang, J. Görres, A. Kontos, Q. Li, S. N. Liddick, A. Long, S. Lyons, K. Padmanabhan, J. Peace, A. Roberts, D. Robertson, K. Smith, M. K. Smith, E. Stech, B. Stefanek, W. P. Tan, X. D. Tang, and M. Wiescher, Nucl. Instrum. Methods Phys. Res., Sect. A **703**, 16 (2013).
[32] C. J. Prokop, S. N. Liddick, B. L. Abromeit, A. T. Chemey, N. R. Larson, S. Suchyta, and J. R. Tompkins, Nucl. Instrum. Methods Phys. Res., Sect. A **741**, 163 (2014).
[33] A. Spyrou, S. N. Liddick, A. C. Larsen, M. Guttormsen, K. Cooper, A. C. Dombos, D. J. Morrissey, F. Naqvi, G. Perdikakis, S. J. Quinn, T. Renstrøm, J. A. Rodriguez, A. Simon, C. S. Sumithrarachchi, and R. G. T. Zegers, Phys. Rev. Lett. **113**, 232502 (2014).
[34] D. Cano-Ott, J. Tain, A. Gadea, B. Rubio, L. Batist, M. Karny, and E. Roeckl, Nucl. Instrum. Methods Phys. Res., Sect. A **430**, 333 (1999).
[35] M. Wang, G. Audi, A. Wapstra, F. Kondev, M. MacCormick, X. Xu, and B. Pfeiffer, Chin. Phys. C **36**, 1603 (2012).
[36] S. Agostinelli, J. Allison, K. Amako, J. Apostolakis, H. Araujo, P. Arce, M. Asai, D. Axen, S. Banerjee, G. Barrand, F. Behner, L. Bellagamba, J. Boudreau, L. Broglia, A. Brunengo, H. Burkhardt, S. Chauvie, J. Chuma, R. Chytracek, G. Cooperman, G. Cosmo, P. Degtyarenko, A. Dell'Acqua, G. Depaola, D. Dietrich, R. Enami, A. Feliciello, C. Ferguson, H. Fesefeldt, G. Folger, F. Foppiano, A. Forti, S. Garelli, S. Giani, R. Giannitrapani, D. Gibin, J. J. G. Cadenas, I. González, G. G. Abril, G. Greeniaus, W. Greiner, V. Grichine, A. Grossheim, S. Guatelli, P. Gumplinger, R. Hamatsu, K. Hashimoto, H. Hasui, A. Heikkinen, A. Howard, V. Ivanchenko, A. Johnson, F. W. Jones, J. Kallenbach, N. Kanaya, M. Kawabata, Y. Kawabata, M. Kawaguti, S. Kelner, P. Kent, A. Kimura, T. Kodama, R. Kokoulin, M. Kossov, H. Kurashige, E. Lamanna, T. Lampén, V. Lara, V. Lefebure, F. Lei, M. Liendl, W. Lockman, F. Longo, S. Magni, M. Maire, E. Medernach, K. Minamimoto, P. M. de Freitas, Y. Morita, K. Murakami, M. Nagamatu, R. Nartallo, P. Nieminen, T. Nishimura, K. Ohtsubo, M. Okamura, S. O'Neale, Y. Oohata, K. Paech, J. Perl, A. Pfeiffer, M. G. Pia, F. Ranjard, A. Rybin, S. Sadilov, E. D. Salvo, G. Santin, T. Sasaki, N. Savvas, Y. Sawada, S. Scherer, S. Sei, V. Sirotenko, D. Smith, N. Starkov, H. Stoecker, J. Sulkimo, M. Takahata, S. Tanaka, E. Tcherniaev, E. S. Tehrani, M. Tropeano, P. Truscott, H. Uno, L. Urban, P. Urban, M. Verderi, A. Walkden, W. Wander, H. Weber, J. P. Wellisch, T. Wenaus, D. C. Williams, D. Wright, T. Yamada, H. Yoshida, and D. Zschiesche, Nucl. Instrum. Methods Phys. Res., Sect. A **506**, 250 (2003).
[37] B. Singh, Nucl. Data Sheets **74**, 63 (1995).
[38] P. Venkataramaiah, K. Gopala, A. Basavaraju, S. S. Suryanarayana, and H. Sanjeeviah, J. Phys. G **11**, 359 (1985).
[39] D. C. Camp and B. P. Foster, Nucl. Phys. A **177**, 401 (1971).
[40] K. Takahashi, T. Kuroyanagi, H. Yuta, K. Kotajima, K. Nagatani, and H. Morinaga, J. Phys. Soc. Jpn. **16**, 1664 (1961).
[41] B. Grapengiesser, E. Lund, and G. Rudstam, J. Inorg. Nucl. Chem. **36**, 2409 (1974).
[42] H. W. Taylor, D. A. Craig, B. Singh, and D. A. Viggars, Int. J. Appl. Radiation Isotopes **36**, 89 (1985).
[43] B. A. Brown and W. D. M. Rae, Nucl. Data Sheets **120**, 115 (2014).
[44] M. Honma, T. Otsuka, T. Mizusaki, and M. Hjorth-Jensen, Phys. Rev. C **80**, 064323 (2009).
[45] B. A. Brown (private communication); and Ref. 28 of B. Cheal *et al.*, Phys. Rev. Lett. **104**, 250501 (2010).
[46] E. Mané, B. Cheal, J. Billowes, M. L. Bissell, K. Blaum, F. C. Charlwood, K. T. Flanagan, D. H. Forest, C. Geppert, M. Kowalska, A. Krieger, J. Krämer, I. D. Moore, R. Neugart, G. Neyens, W. Nörtershäuser, M. M. Rajabali, R. Sánchez, M. Schug, H. H. Stroke, P. Vingerhoets, D. T. Yordanov, and M. Žáková, Phys. Rev. C **84**, 024303 (2011).
[47] D.-L. Fang and B. A. Brown (unpublished).
[48] J. C. Hardy and I. S. Towner, Nucl. Phys. News **16**, 11 (2006).
[49] J. C. Hardy and I. S. Towner, Phys. Rev. C **79**, 055502 (2009).
[50] N. Gove and M. Martin, At. Data Nucl. Data Tables **10**, 205 (1971).